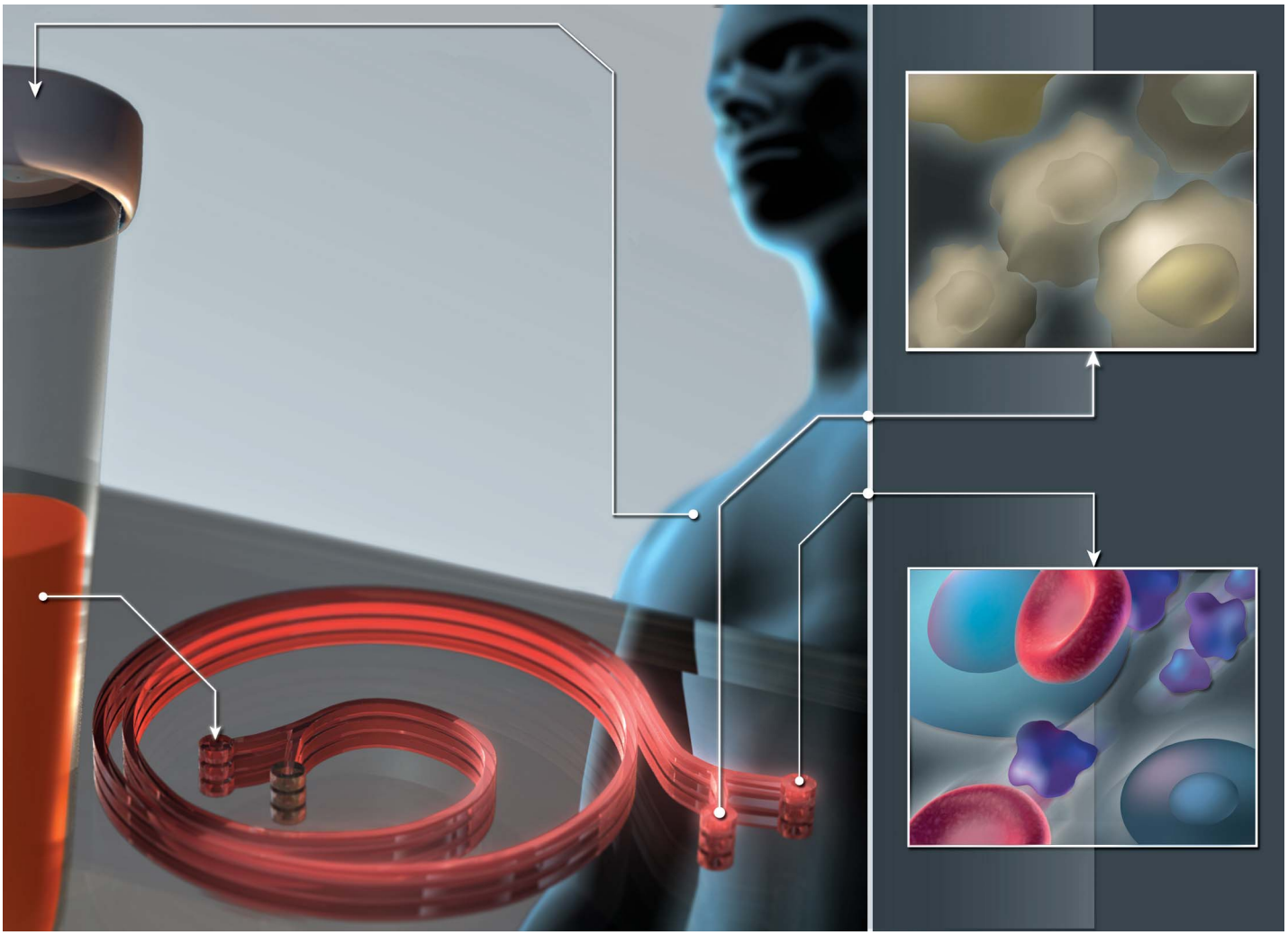

Showcasing research on the detection and retrieval of clinical circulating tumor cells from peripheral blood of cancer patients using spiral microfluidics from the team of Professor Chwee Teck Lim at the Department of Biomedical Engineering and the Mechanobiology Institute, National University of Singapore, and Professor Jongyoon Han at the Singapore–MIT Alliance for Research and Technology (SMART), Singapore. (Artwork by Larisa Bulavina from the Mechanobiology Institute, National University of Singapore.)

Title: An ultra-high-throughput spiral microfluidic biochip for the enrichment of circulating tumor cells

Using the spiral microfluidic biochip to detect and characterize rare circulating tumor cells from the blood of cancer patients can not only provide critical insights into tumor biology, but also hold great promise for cancer diagnosis, prognosis and treatment.

As featured in:

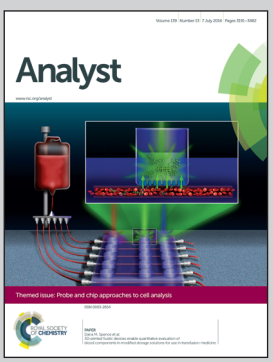

See Jongyoon Han, Chwee Teck Lim *et al.*, *Analyst*, 2014, **139**, 3245.

ROYAL SOCIETY OF CHEMISTRY

www.rsc.org/analyst

Registered charity number: 207890

Analyst

PAPER

View Article Online
View Journal | View Issue

Cite this: *Analyst*, 2014, **139**, 3245

An ultra-high-throughput spiral microfluidic biochip for the enrichment of circulating tumor cells†

Majid Ebrahimi Warkiani,‡[a] Bee Luan Khoo,‡[bc] Daniel Shao-Weng Tan,[d] Ali Asgar S. Bhagat,[e] Wan-Teck Lim,[d] Yoon Sim Yap,[d] Soo Chin Lee,[f] Ross A. Soo,[f] Jongyoon Han*[ag] and Chwee Teck Lim*[abc]

The detection and characterization of rare circulating tumor cells (CTCs) from the blood of cancer patients can potentially provide critical insights into tumor biology and hold great promise for cancer management. The ability to collect a large number of viable CTCs for various downstream assays such as quantitative measurements of specific biomarkers or targeted somatic mutation analysis is increasingly important in medical oncology. Here, we present a simple yet reliable microfluidic device for the ultra-high-throughput, label-free, size-based isolation of CTCs from clinically relevant blood volumes. The fast processing time of the technique (7.5 mL blood in less than 10 min) and the ability to collect more CTCs from larger blood volumes lends itself to a broad range of potential genomic and transcriptomic applications. A critical advantage of this protocol is the ability to return all fractions of blood (*i.e.*, plasma (centrifugation), CTCs and white blood cells (WBCs) (size-based sorting)) that can be utilized for diverse biomarker studies or time-sensitive molecular assays such as qRT-PCR. The clinical use of this biochip was demonstrated by detecting CTCs from 100% (10/10) of blood samples collected from patients with advanced-stage metastatic breast and lung cancers. The CTC recovery rate ranged from 20 to 135 CTCs mL^{-1} and obtained under high purity (of 1 CTC out of every 30–100 WBCs which gives ~4 log depletion of WBCs). They were identified with immunofluorescence assays (pan-cytokeratin+/CD45−) and molecular probes such as HER2/*neu*.

Received 19th February 2014
Accepted 9th April 2014

DOI: 10.1039/c4an00355a

www.rsc.org/analyst

Introduction

Circulating tumor cells (CTCs), cancer cells of solid tumor origin that shed into the blood stream from either primary or secondary tumors of patients, directly contribute to the haematogenous metastatic spread and subsequent growth of tumor cells at distant sites within the body.[1,2] The isolation and recovery of these CTCs is very challenging, primarily due to their rarity in peripheral blood and also their heterogeneity.[3] Nevertheless, the enrichment of CTCs can help clinicians better understand the biology of metastasis and disease progression as well as contribute to cancer management by potentially serving as a powerful clinical prognostic tool and non-invasive analysis of tumor genotypes for the therapeutic management of cancer-related diseases.[3,4] However, conventional clinical approaches for isolation of CTCs from peripheral blood, including flow cytometry,[5] gradient centrifugation,[6] and fluorescence and magnetic-activated cell sorting,[7,8] are often based on antigen recognition techniques, which are expensive and limited in yield and purity. Most techniques require long processing times, resulting in low cell viability of the enriched CTCs. They also do not allow complete fractionation and preservation of plasma, white blood cells (WBCs) and CTCs. A reliable method for the rapid, efficient and effective enrichment of CTCs will therefore be pivotal for deepening our understanding of the metastatic process and contribute to the field of clinical oncology.

Microfluidics is one of the most rapidly developing technologies for innovation in cancer research. The application of microfluidic systems for the separation of CTCs provides unprecedented opportunities for efficient enrichments of these

[a]*BioSystems and Micromechanics (BioSyM) IRG, Singapore-MIT Alliance for Research and Technology (SMART) Centre, Singapore*
[b]*Mechanobiology Institute, National University of Singapore, Singapore*
[c]*Department of Biomedical Engineering, National University of Singapore, 9 Engineering Drive 1, Singapore 117575, Singapore. E-mail: ctlim@nus.edu.sg*
[d]*Department of Medical Oncology, National Cancer Centre Singapore, Singapore*
[e]*Clearbridge BioMedics Pte Ltd, Singapore*
[f]*Department of Hematology-Oncology, National University Hospital, Singapore*
[g]*Department of Electrical Engineering and Computer Science, Department of Biological Engineering, Research Laboratory of Electronics, Massachusetts Institute of Technology, Room 36-841, 77 Massachusetts Avenue, Cambridge, MA 02139, USA. E-mail: jyhan@mit.edu*

† Electronic supplementary information (ESI) available. See DOI: 10.1039/c4an00355a

‡ These authors contributed equally to this paper.

rare cells from blood, allowing detailed molecular characterization of them at the single-cell level.[9] While several microfluidic devices have been reported for the isolation of CTCs using epithelial cell surface antigens such as EpCAM (epithelial cell adhesion molecule),[10,11] these platforms/techniques rely on mediating the interaction of target CTCs with anti-EpCAM antibody-coated features including micropillars[10] or nanoporous surfaces[12] under precisely controlled laminar conditions with reliable efficiency. However, some tumor cells express low or no EpCAM (*e.g.*, for cells that undergo epithelial–mesenchymal transition (EMT)), resulting in incomplete retrieval of CTCs.[1,13] In addition, the immunomagnetic isolation approaches involve biochemical manipulation of the cells, rendering them non-viable or challenging for culture as well as for downstream molecular analysis.[14,15] To date, a number of microfluidic devices that employ dielectrophoretic forces have also been developed for isolation of cancer cells based on differences in responses of the cells to the electric field.[14,16,17] Although this allows for label-free cell sorting without relying on immunochemistry, this technique is limited due to the subtle dielectric differences between CTCs and blood cells, thereby affecting the throughput and purity and the high electric fields that can potentially cause gene expression (phenotypic) changes.[18] To overcome the above limitations, cell size and deformability have been exploited in order to isolate CTCs from blood. Most CTCs are believed to be larger than the other blood components (<20 μm) (RBCs, peripheral WBCs and platelets),[19,20] including tumor cells obtained from small cell lung cancer patients.[21] This obviates the need for any prior knowledge of the target cells' biochemical characteristics, while enabling collection of putative CTCs regardless of their EpCAM expression. The most popular size/deformability-based CTC isolation methods rely on using either track-etched membranes or microfabricated filters.[22,23] These techniques are limited by the volume of blood that can be processed due to issues arising from filter clogging, low recovery, low purity and low cell viability due to cell damage caused by high shear incurred as the cells are made to pass through the filter pores.

Hydrodynamic filtration systems for size-based separation in the microfluidic devices can overcome these shortcomings of the current approaches including clogging, low recovery and cell viability issues.[24,25] The controlled laminar flow within microfluidic channels can be manipulated to generate size-dependent cell trajectories for high-resolution CTC enrichment. Previously, we reported a novel microfluidic platform for blood fractionation (also known as '*Dean Flow Fractionation*') and applied it successfully for isolation of CTCs from whole blood.[25,26] We have shown that the integrated spiral biochip is capable of processing blood with a hematocrit of 20–25%, thus allowing processing and enrichment of rare cells with speed of ~3 mL h^{-1}. Herein, we report the development of a simple yet reliable multiplexed spiral biochip for the ultra-high-throughput isolation, label-free isolation of CTCs to address the challenges of the next generation CTC enrichment platform such as *high sensitivity* (near 100% detection rate), *high purity* (~750 WBCs mL^{-1}), *high-throughput* (7.5 mL in less than 10 min), *label-free* enrichment, *simplicity* and *ease of operation*. In contrast to the previous version, this device can work with a minimum of two syringe pumps instead of three (*i.e.*, making automation easier) and can process a larger volume of blood samples in a shorter time with relatively higher sensitivity and purity. Processing a larger volume of blood samples can boost the number of enriched CTCs for multiple downstream assays such as immunofluorescent staining, quantitative RT-PCR (qRT-PCR), fluorescence *in situ* hybridization (FISH) and also time-sensitive molecular tests such as RNA-sequencing. The clinical use of this biochip was demonstrated by the isolation of CTCs from 100% (10/10) of blood samples collected from patients with advanced-stage metastatic breast and lung cancer. Retrieved cells are unlabelled and hence more viable for propagation, drug development tests and other downstream analyses. This design is ideal for the development of a low-cost and automated CTC detection-and-retrieval device for cancer diagnosis and prognosis.

Materials and methods

Device fabrication

SU-8 silicon molds were fabricated using standard lithography techniques.[27,28] The patterned silicon wafer was silanized with trichloro (1*H*,1*H*,2*H*,2*H*-perfluorooctyl) silane (Sigma Aldrich, USA) to render the surface hydrophobic. PDMS prepolymer was prepared by mixing the PDMS at a standard 1 : 10 ratio (Sylgard 184, Dow Corning, USA) and degassing in a vacuum chamber. To produce the single-layer spiral biochip, PDMS prepolymer was poured onto the SU-8 mold and cured at 80 °C for 1–2 h inside a conventional oven. The PDMS was then cut from the mold, and four fluidic access holes (two inlets and two outlets) were punched. In order to obtain the multiplexed device, three spiral biochips were bonded together using oxygen plasma and manual alignments. The final device was obtained by bonding the whole assembly onto a microscopic glass slide using an air plasma machine.

Cell culture and sample preparation

Two commercially available human cancer cell lines, namely breast adenocarcinoma (MCF-7) and bladder (T24) were first used to mimic CTC separation. The MCF-7 cells (HTB-22™, ATCC, USA) and T24 cells (HTB-4™ ATCC, USA) were cultured in high-glucose Dulbecco's modified Eagle's medium (DMEM) (Invitrogen, USA) supplemented with 10% fetal bovine serum (FBS) (Invitrogen, USA) together with 1% penicillin–streptomycin (Invitrogen, USA). The culture was maintained at 37 °C in a humidified atmosphere containing 5% (v/v) CO_2 until 80% confluence. Cells were cultured in sterile 6-well plates (BD Bioscience, USA) and sub-cultivated (1 : 3) twice a week with media replaced every 48 h. Sub-confluent monolayers were dissociated using 0.01% trypsin and 5.3 mM EDTA solution (Lonza, Switzerland). For the control and recovery experiments, the cancer cells were diluted in buffer containing 1× phosphate buffered saline (PBS), 2 mM ethylenediaminetetraacetic acid (EDTA) supplemented with 0.5% bovine serum albumin (BSA) (Miltenyi Biotec, Germany) to prevent non-specific adsorption on the tubing and microchannel walls. For all experiments

unless otherwise mentioned, whole blood obtained from healthy donors was lysed using red blood cell (RBC) lysis buffer (Bioscience, USA) for 5 min at room temperature under continuous gentle mixing. The lysed RBCs were removed by centrifugation at 1000×*g* for 5 min and the nucleated cell fraction was re-suspended in phosphate buffered saline (PBS) accordingly. The process of RBC lysis removes blood contaminants and hence reduces the overall cell concentration. Therefore, nucleated cells can be resuspended in a smaller volume of buffer, speeding up the process of size-based sorting by the microfluidic device.

Immunofluorescence staining and Fluorescent Automated Cytometry System (FACS) analysis

Results from experiments conducted to determine the cell loss incurred by lysis were analyzed by performing flow cytometry analysis using a BD Accuri C6 flow cytometer (BD Biosciences, USA) on the lysed and whole blood spiked samples. Samples were spiked with 100,000 T24 cells pre-stained with fluorescein isothiocyanate (FITC)-conjugated pan-cytokeratin (CK) antibody (1 : 100, Miltenyi Biotec Asia Pacific, Singapore). Outlet samples were concentrated to 1 mL and processed for quantification of pan-CK+ cells. For quantification of cell counts, immunofluorescence (IF) staining was carried out to allow visualization and differentiation of the various cell types. The outlet samples were fixed with 4% paraformaldehyde (PFA) (Sigma, USA) for 10 min at room temperature, permeabilized with 0.1% Triton X-100 in PBS (Sigma, USA). Permeabilized cells were treated with an antibody cocktail (pan-CK antibody, APC-conjugated CD45 antibody (1 : 100), Miltenyi Biotec Asia Pacific, Singapore) and Hoechst dye in PBS buffer for 30 min on ice. During flow cytometry analysis, the cells were gated based on the forward and side scatters as well as the fluorescence intensity.

Viability culture experiments

A known concentration of T24 cells were spiked into whole blood before lysis. T24 cell counts (before and after lysis) were compared by enumeration of recovered T24-spiked blood after their respective treatment. Recovered cells were seeded onto 2D substrates under optimal growth conditions and bright field images were obtained after 5 min from seeding.

DNA fluorescence *in situ* hybridization (FISH)

Samples were obtained from patients with HER2+ tumor status. The tumors were extracted *via* biopsy in the diagnostic stage (pre-treatment) and analysed for gene amplification *via* PCR in the hospital (not shown). Cells were spun onto slides using a Cytospin centrifuge (Thermo Scientific, USA) at 600 rpm for 6 min. Slides were fixed in 4% PFA at room temperature for 10 min and dehydrated *via* ethanol series (80%, 90%, and 100%). For DNA FISH, slides were treated with RNase (4 mg mL^{-1}) (Sigma, USA) for 40 min at 37 °C, washed with 1× PBS/0.2% Tween 20 (Sigma, USA) thrice and denatured with 70% formamide/2× SCC for 10 min at 80 °C. They were then quench dehydrated again *via* ice-cold ethanol series. HER2 probes were directly applied to slides maintained at 42 °C. Hybridization was continued at 42 °C under dark and humid conditions overnight. Slides were washed with 50% formamide/2× SSC and 2× SSC at 45 °C under shaking, counterstained with 4′,6-diamidino-2-phenylindole (DAPI) and sealed with a 50 mm × 50 mm coverslip (Fisher Scientific, USA).

Clinical samples

Human whole blood samples were obtained from healthy donors and 10 patients with either metastatic lung or breast cancer. This study was approved by our local ethics committee according to a protocol permitted by the Institutional Review Board (IRB). A total of 5 blood samples from healthy donors were used as controls and 10 samples from lung and breast cancer patients were processed for CTC enumeration. Blood samples were collected in Vacutainer® tubes (Becton-Dickinson, Franklin Lakes, NJ, USA) containing EDTA anticoagulant and were processed within 2–4 h to prevent blood coagulation. For all the samples, 7.5 mL of whole blood was lysed initially using RBC lysis buffer and re-suspended in PBS prior to processing on the biochip. 7.5 mL of blood was concentrated to 3.75 mL for processing, reducing the processing time. Samples were processed at an input velocity of 350 μL min^{-1}.

Results and discussion

Working principle

Fig. 1A schematically illustrates the principle of hydrodynamic separation in spiral microfluidic channels. In the spiral microchannels with rectangular cross-section, the influence of centrifugal forces acting in the radial direction results in the formation of two symmetrical counter-rotating vortices across the channel cross-section, also known as Dean vortices. Under Poiseuille flow conditions, naturally buoyant particles of varying sizes equilibrate at different positions along the microchannel cross-section under the influence of inertial lift and Dean drag forces.[24] By confining the cells at the inlet to one region of the channel cross-section, we can effectively fractionate the cells by equilibrating the CTCs near the microchannel inner wall while driving the smaller hematological cells (platelets and WBCs) to the microchannel outer wall, allowing an efficient separation at the outlet.[29] The spiral biochip enriches the CTC population by a significant 10^4-fold from a RBCs-depleted nucleated cell fraction. It consists of two inlets and two outlets to enrich the larger CTCs at the outlet. The collected CTCs can then be analyzed by suitable downstream techniques such as immunostaining, qRT-PCR and FISH or can be employed for culturing and single-cell analysis (Fig. 1B).

Spiral biochip operating parameter optimization

The challenge for clinical use of CTCs is to develop an unbiased, high-throughput and reliable assay to enrich viable CTCs from peripheral blood within a reasonable period of time. High-speed frame capture (6,400 frames per second) of CTC isolation *via* the spiral device is illustrated in Fig. 2A. For all the experiments, high-speed imaging was performed to monitor the

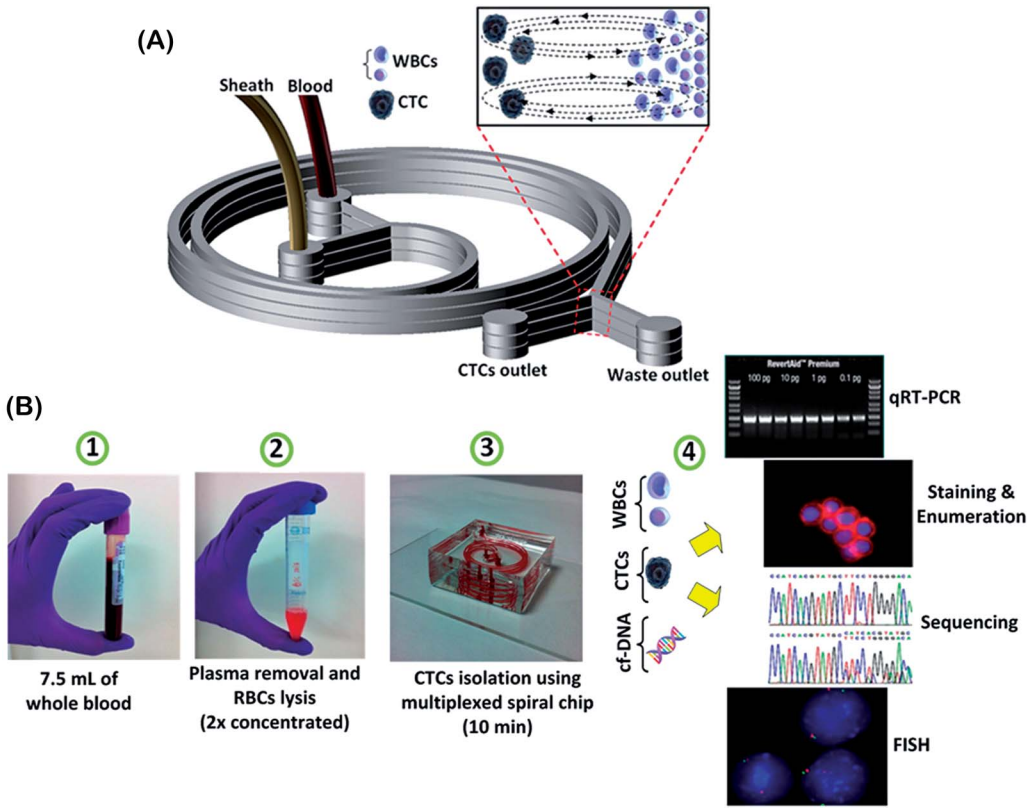

Fig. 1 (A) Schematic representation of the configuration and operation of a multiplexed spiral microfluidic chip for capturing CTCs with two inlets and two outlets. (B) Sample processing workflow showing different steps of enrichment and identification. The blood sample was first collected, RBCs were lysed and processed through a multiplexed spiral biochip. The isolated CTCs were then made available for immunostaining using specific markers or FISH. DNA or RNA can be extracted from the CTCs and subjected to next-generation sequencing and qRT-PCR. Viable cells can be released and propagated in cell culture for various applications including cancer stem cell (CSC) study or drug discovery.

position of CTCs and WBCs near the outlet region (see Movie S1 and S2 in ESI†). 99.99% of WBCs and residual RBCs underwent a complete Dean cycle migration and exited at the waste outlet while CTCs that were focused near the inner wall during the lateral migration can be collected from the CTC outlet. To reduce the amount of cellular components flowing in the spiral biochip, we employed a conventional RBC lysis technique (using ammonium chloride solution) in order to process a larger volume of clinical samples. While WBCs constitute just 1% of the total blood volume fraction, it is still challenging to efficiently separate minute quantities of CTCs from them. Extensive characterization of the proposed methodology was carried out to study the depletion capability of WBCs in the spiral biochip. To demonstrate the impact of input sample cell concentration on the device performance and final purity, we carried out the processing of blood under different nucleated cell concentrations. An initial 7.5 mL of whole blood collected from healthy donors had the RBCs lysed and the nucleated cell fraction was then spun down and resuspended back to 7.5 mL (1× concentration), 3.75 mL (2× concentration) and 2.5 mL (3× concentration), respectively. Fig. 2B shows the total cell count collected from the CTC outlet at different sample concentrations in 5 min. A linear incremental trend in the total cell count is observed, suggesting the effect of the initial WBC concentration on the final purity. Since the total number of WBCs varied from one patient to another and with cancer type/stage,[30] we decided to use a 2× concentration (~14×10^6 WBCs) as optimal for future tests and clinical validation. This translates to a total processing time of around 10 min for a 7.5 mL blood sample using a multiplexed device with three stacked spiral biochips (see Fig. 1).

Next, to demonstrate robustness and repeatability, a pure population of leukocytes was processed through the biochip at 2× concentration continuously. Enriched samples containing the contaminating WBCs were collected from the CTC outlet for a period of 5 min, each collection taken from different time intervals (0–5, 5–10 and 10–15 min) from the start of processing. The WBC count collected at the different time points is fairly uniform with approximately 900–1200 cells collected under the optimal flow conditions (see Fig. 2C). Microscopic analysis of the collected WBCs (data not shown) revealed that this subpopulation was in the order of CTCs in terms of size (*i.e.*, ~12–15 μm), and can be easily differentiated using immunofluorescence staining and molecular approaches. Starting with an initial concentration of ~7×10^6 nucleated cells, the spiral biochip depleted ~99.99% of the WBCs, providing a purer CTC fraction at the outlet. This is particularly important for many downstream molecular assays where the contaminating

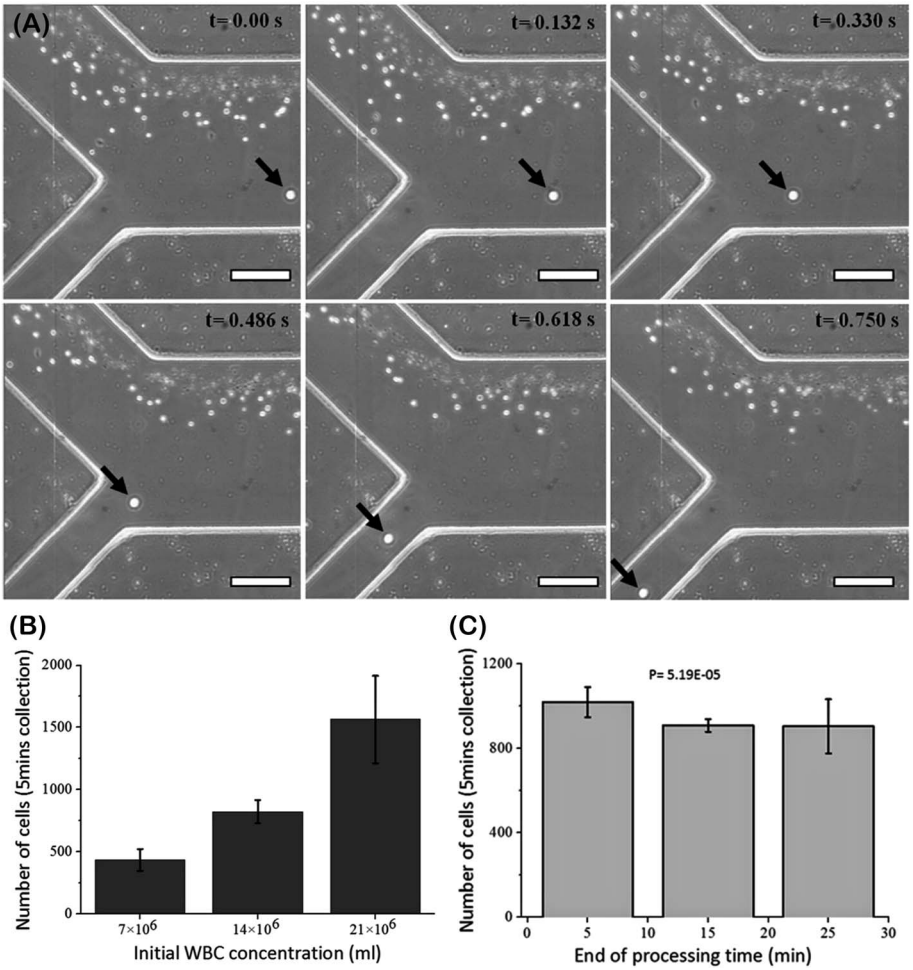

Fig. 2 (A) Time sequence images demonstrating the isolation of rare cells using the spiral microfluidic biochip. Taking advantage of the inherent secondary Dean vortex flows present in curvilinear microchannels, the CTCs (marked with a black arrow) can be focused near the microchannel inner wall while driving the smaller hematological cells (RBCs and WBCs) toward the microchannel outer wall, thus allowing an efficient separation at the outlet. Scale bar is 100 μm. (B) Different WBC concentrations affect the total number of nucleated cells collected at the first 5 min of processing ($n = 3$; Anova (single factor), $P < 0.05$). (C) Linear increase in nucleated cells isolated along with the respective increase in whole blood processed under 2× concentration. This demonstrates the relatively constant rate of nucleated cell collection with time. ($n = 3$; Anova (single factor), $P < 0.05$.)

materials from WBCs can significantly lower the signal-to-noise ratio, leading to inaccurate diagnosis.

Effect of RBC lysis on separation efficiency and cell viability

Chemical lysis of whole blood using ammonium chloride has been employed extensively for the depletion of contaminated RBCs in various applications such as transcriptome analysis of WBCs in various human diseases. While some people have reported that RBC lysis can lead to compounded loss of cells,[30] we have shown here that depletion of RBCs did not significantly compromise the recovery and isolation of cancer cells (Fig. 3A). Exposure to the lysis buffer also did not alter the morphology and size of the cells (Fig. 3B).

We also compared the performance of our previous integrated biochip[26] with the new multiplexed spiral one for CTC isolation. In the previous integrated biochip, whole blood was processed (100 μL min^{-1}) with the two-biochip cascaded spiral device and progressively diluted with a sheath flow (750 μL min^{-1}) running through the device. 7.5 mL of whole blood is processed in about 30 min. The CTC counts obtained from both biochips where they were used for the analysis of samples from lung cancer patients are shown in Fig. 3C. The multiplexed spiral biochip yielded a significantly improved capture efficiency in comparison with the previous integrated biochip which processed whole blood. This is also done under a shorter time (7.5 mL of blood in 10 min), giving rise to a much higher throughput (Fig. 3D). In addition, the purity of retrieved CTCs captured among contaminating WBCs was significantly higher for the multiplexed biochip, compared with the integrated one.

Isolation efficiency and cell viability using cancer cell lines

To test the performance of the multiplexed spiral biochip for CTC isolation and recovery, we characterized the biochip with commercially available cancer cell lines. Cell lines have been

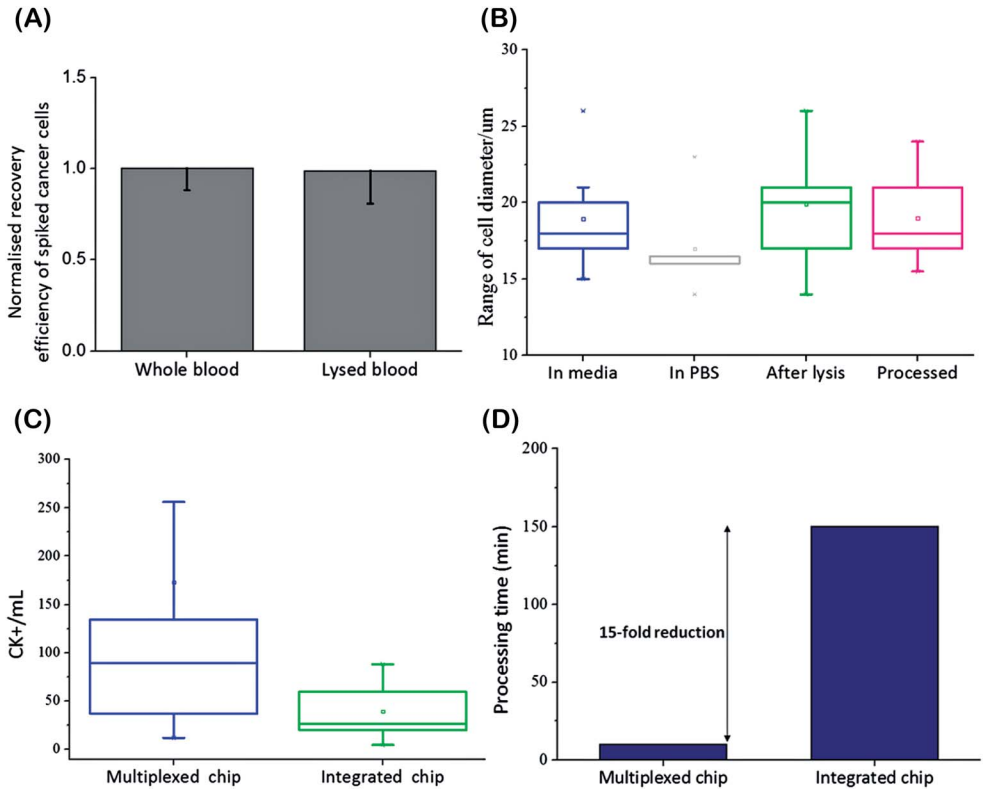

Fig. 3 (A) Minimal cell loss incurred upon cell lysis. Flow cytometry quantification for recovery of spiked T24 cells was comparable to that enumerated for recovery of cells spiked in whole blood (98% with respect to recovery in whole blood) ($n = 3$; Anova, $P = 0.82$). (B) Range of MCF-7 cell diameters after exposure to different media. No significant increase in cell diameter was detected ($n = 3$; Anova, $P = 0.2$). (C) CTC count obtained by the integrated spiral biochip was compared against that of the current multiplexed spiral using the blood of patients with lung cancer. (D) Sample processing time by the integrated spiral biochip was compared with that of the current multiplexed spiral biochip (*i.e.*, for 7.5 mL of blood).

shown to be a good surrogate for characterization of various microfluidics as well as other CTC enrichment assays. Using the spiral biochip, we demonstrated the high recovery of breast (MCF-7) and bladder (T24) cancer cells spiked into healthy blood samples. These cell lines were chosen due to their different range of cell diameters (MCF-7: ~20 μm; T24: ~30 μm), which validated the ability of the multiplexed spiral biochip for enriching CTCs of different sizes from various cancer types. Following enrichment, cancer cells were identified by immunofluorescence staining either by enumerating under epi-fluorescence microscopy or by flow cytometry analysis with common biomarkers (CK+/CD45−). For both cell lines spiked at clinically relevant concentrations of 500 cells per 7.5 mL of whole blood, a recovery of 87.6% for MCF-7 and 76.4% for T24 cells was achieved (Fig. 4A).

To verify cell viability, propidium iodide (PI) staining of recovered samples was performed. High viability was confirmed by the minimal staining (<10%) detected by flow cytometry (Fig. 4B). Viable cells isolated can then be seeded onto 2-D culture substrates, where they attach and proliferate under standard culture conditions. The morphology of the cells remained relatively unchanged at different stages of processing (before lysis, after lysis and after processing with lysis (see Fig. 4C)). Isolated cells after device processing also remain viable for days after seeding onto culture substrates (see ESI Fig. S1†). This illustrates that both the lysis process and the shear force induced during retrieval did not affect the cell viability, and is in good agreement with previous studies showing that the high shear conditions inside the spiral microchannels have no adverse effects on the enriched cells.[31]

Enrichment of CTCs from patients with metastatic breast and lung cancer

Using the optimal test parameters, 7.5 mL blood samples from 5 healthy volunteers (control) and 5 patients with metastatic breast cancer and 5 patients with non-small cell lung cancer (NSCLC) were processed (Table 1). CTCs captured by the spiral biochip were identified using a comprehensive image analysis algorithm, consisting of staining with Hoechst for DNA content, FITC-conjugated pan-cytokeratin antibodies for cancer/epithelial cells, and APC-conjugated anti-CD45 antibodies for haematological cells (Fig. 5B). Cells stained positive for both Hoechst and pan-cytokeratin whereas negative for CD45 were scored as CTCs. CTCs were detected in 10 of 10 patient samples (100% detection) with counts ranging from 20 to 67 CTCs mL^{-1} for breast cancer samples and 33 to 135 CTCs mL^{-1} for lung cancer samples (Fig. 5A). CTC diameter ranges were from 15–25 μm for lung cancer samples and 20–35 μm for breast cancer

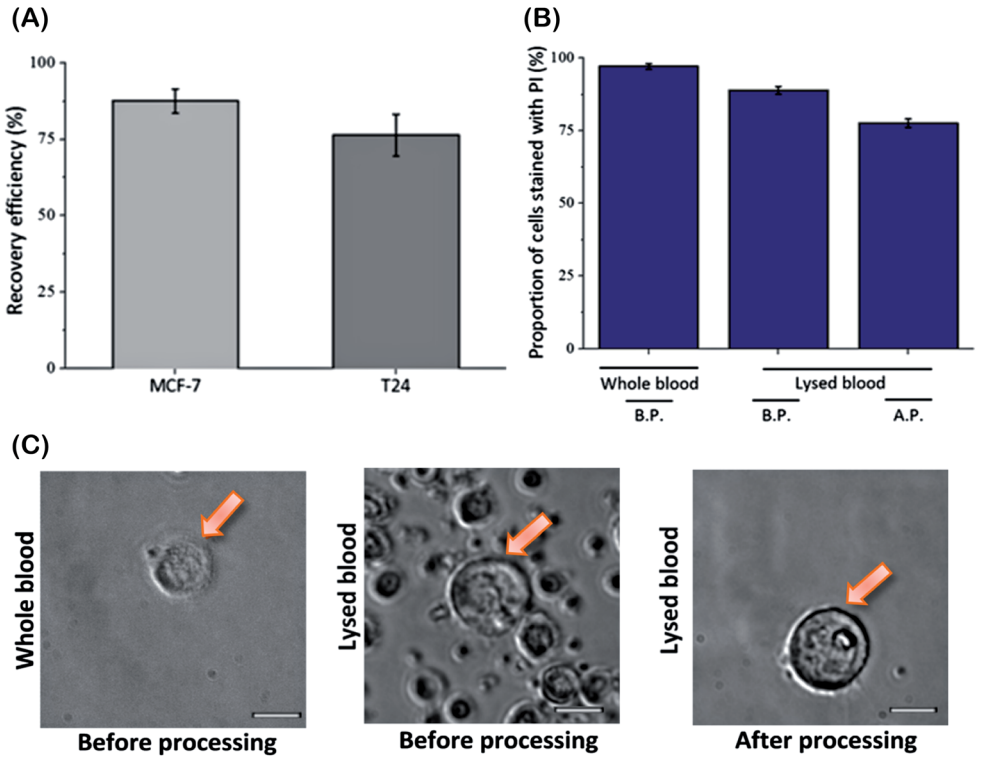

Fig. 4 (A) Recovery of spiked cancer cells introduced at clinically relevant concentration (500 cells per 7.5 mL whole blood) ($n = 3$; Anova (single factor), $P < 0.05$). (B) Proportion of viable cells after various treatments, as stained by propidium iodide (B.P.: before processing; A.P.: after processing). (C) Phase contrast microscopy images of isolated T24 cells at different treatment conditions. The morphology of the cells remained relatively constant after lysis and spiral processing treatments, and cells remained viable. Cancer cells are indicated by orange arrows. Scale bar is 10 μm.

samples (data not shown). Epithelial cells positive for pan-cytokeratin were also detected in healthy volunteers (1–4 mL^{-1}), indicating a clear detection threshold.

To assess the feasibility of characterizing gene copy number alteration by FISH of CTCs isolated using the multiplexed spiral biochip, we have selected a few HER2-positive breast cancer samples for analysis. These samples were obtained from patients with HER2-positive tumor status. HER2-positive breast cancer has been reported to be more aggressive than other types of breast cancer;[32,33] however, treatments that specifically target

Table 1 Clinico-pathological characteristics of patients enrolled in this study for CTC enumeration (C: cycle, D: day, Sutent®: sunitinib)

Sample no	Subject status	CK+ cells mL^{-1}	Cancer stage	Treatment timepoint
1	Healthy	1	N.A.	N.A.
2	Healthy	3	N.A.	N.A.
3	Healthy	3	N.A.	N.A.
4	Healthy	4	N.A.	N.A.
5	Healthy	2	N.A.	N.A.
1	Breast	20	IV	C1D15
2	Breast	61	IV	Post-Sutent®
3	Breast	55	IV	C1D15
4	Breast	34	IV	Baseline
5	Breast	67		Baseline
1	Lung	33	IV	Single draw
2	Lung	43	IV	Single draw
3	Lung	37	IV	Single draw
4	Lung	90	IV	Single draw
5	Lung	135	IV	Single draw

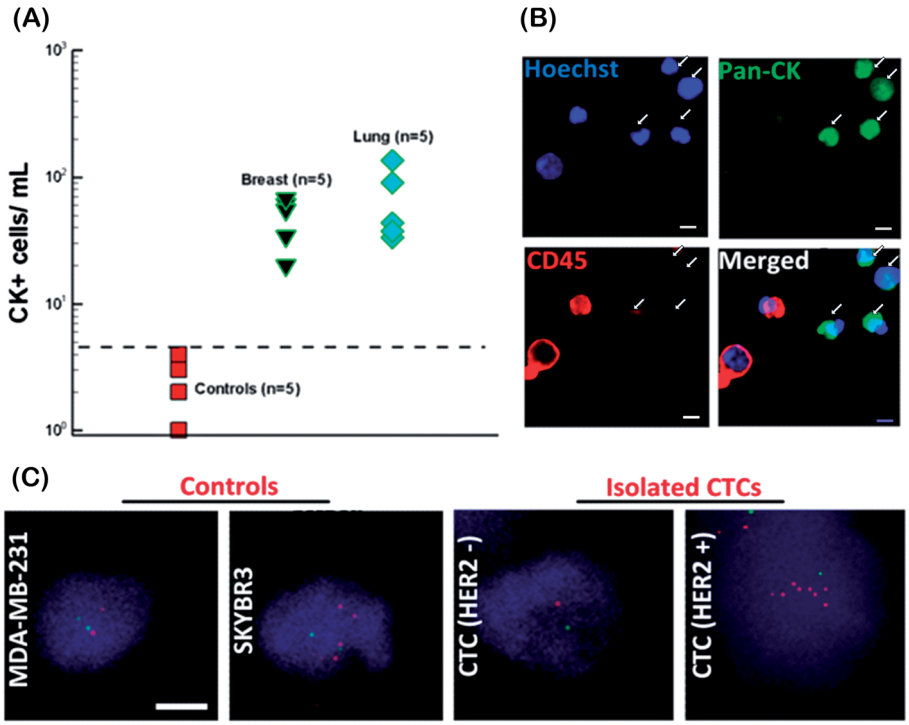

Fig. 5 Enumeration of CTCs from cancer patients. (A) Plot of CTC enumeration for healthy donors (red), breast cancer patients (black) and lung cancer patients (blue). (B) Immunofluorescence staining of isolated CTCs. CTCs (marked by white arrow) were identified by the following criteria: Hoechst positive, pan-cytokeratin positive and CD45 negative. Scale bar is 16 μm. (C) FISH for HER2 detection for breast cancer cell line MDA-MB-231, SKBR3 and breast CTCs enriched by the multiplexed spiral chip. Nuclei of cells were stained with DAPI, HER-2/*neu* gene locus (red) and chromosome 17 centromere (CEP 17) (green). Scale bar is 10 μm.

HER2 are very effective.[34] HER2 signals in isolated CTCs were compared against control breast cancer cell lines SKBR3 (amplified HER2 signals) and MDA-MB-231 (non-amplified HER2 signal) as shown in Fig. 5C. Intriguingly, we found that the HER2 status on isolated CTCs did not correlate with primary tumor characteristics. For 3 (out of 5) patients that were analyzed in this study, the HER2 status was negative (where amplified HER2 expression was determined when the ratio of HER2/centromere of chromosome 17 (Cen17) signals in single nuclei was >2), indicating the heterogeneity of HER2 status in disseminated cells and primary tumor.

Pleomorphism and heterogeneity of enriched CK+ cells

Collected CTCs demonstrated intrapatient pleomorphism. Complementing immunofluorescence staining with epifluorescence microscopy detection, we observed differences in cell and nuclear morphology, nuclear-to-cytoplasmic (N/C) ratios and staining pattern. Stained CTCs isolated from the spiral biochip revealed distinct pleomorphic cell types, as shown from the images of the CTCs provided (Fig. 6A). The CTCs varied from cells densely stained at the nucleus and showed eccentric nuclear morphology, to those which had a bi-lobed or even kidney-shaped nucleus. Such variation in nuclear morphology has also been previously reported.[35] The CTC size also differs with diverse N/C ratios. In some samples, CTC microemboli (clusters) were also observed. In order to further characterise these cells, CTCs were stained for CD166 and CD133, identifying a rare sub-population (~1 in 135 cells) (Fig. 6B). CD166 and CD133 are putative cancer stem cell biomarkers that have been associated with tumor progression, poor patient survival and early tumor relapse.[36,37]

Discussion

Despite recent technological advances, the development of a simple and robust platform capable of enriching CTCs with high throughput (*i.e.*, processing clinically relevant blood volumes within a few minutes), high sensitivity, high specificity, and high cell viability remains elusive. Microfluidic systems for separation of CTCs provide unprecedented opportunities for the efficient enrichment of these rare cells from blood, allowing detailed molecular characterization of them at the single-cell level. Previously, we developed a spiral microfluidic biochip for blood fractionation and applied it successfully for size-based isolation of CTCs from blood.[26] The integrated biochip developed was capable of processing blood with a high hematocrit (~20–25%), thus allowing processing and enrichment of tumor cells at speed of ~3 mL h^{-1}. However, a reduction in processing time will help translate our previous platform to in-clinic and 'point-of-care' applications. Here, we demonstrate the application of a multiplexed spiral biochip for ultra-high-throughput isolation of CTCs from lysed blood using inertial focusing microfluidics to realize a single-step label-free enrichment process. This device is capable of efficient cell separation of clinically relevant blood volumes within a short period of time

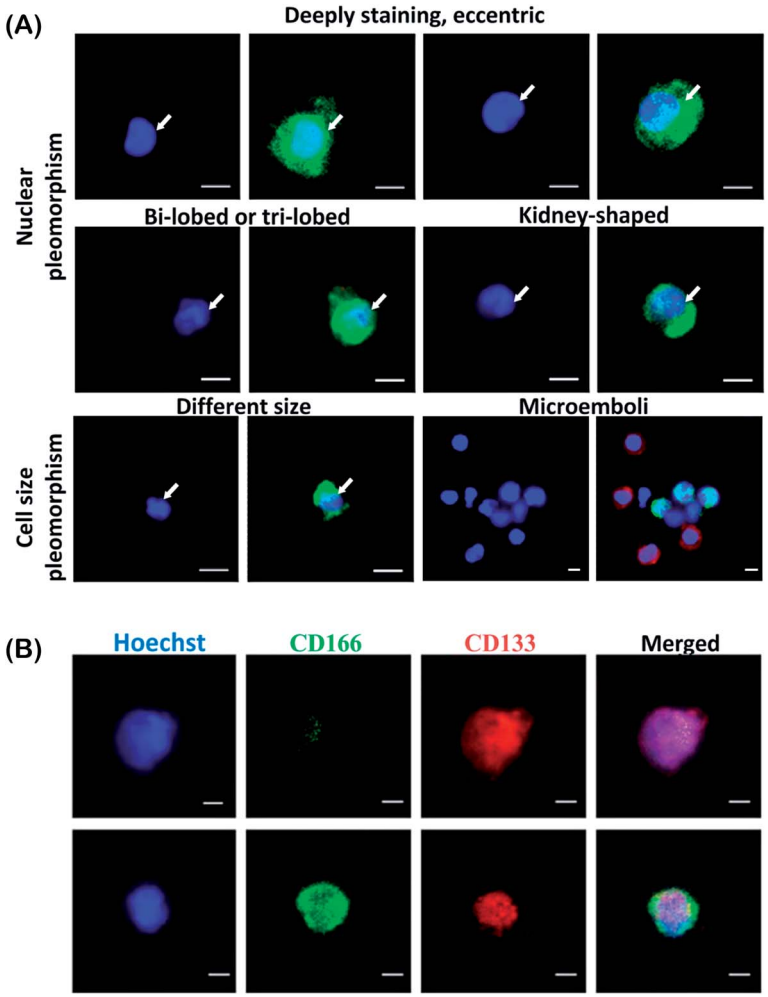

Fig. 6 (A) CTC nuclear and cell size pleomorphism. Isolated CTCs displayed a varied range of nuclear shapes and cell sizes (blue: Hoechst; green: CK). (B) Staining for stem cell markers on lung CTCs. Populations of CD166+ cells were rare in most of the samples. In some instances, some CD166+/CD133+ cells were also detected in certain samples. Scale bar is 10 μm.

(7.5 mL blood in 10 min), thus allowing isolation of viable CTCs with high sensitivity and purity. Compared with other microfluidics-based methods, this device has the following merits. (i) *High-throughput processing*: by stacking up a number of biochips, we can further increase the throughput to handle larger sample volumes and accommodate more downstream assays. (ii) *Simplicity and ease of operation*: the simple design of the spiral biochip with large channel dimensions prevents clogging and facilitates multiplexing and automation for quick translation for diagnostic/prognostic purposes. The simplicity in manufacturing (*i.e.*, no pretreatment or antibody immobilization required) of the device and its ease of operation make it attractive for clinical applications requiring one-time-use operation. The multiplexed spiral biochip demonstrates high sensitivity by the successful detection and isolation of CTCs from 100% (10/10) blood samples collected from patients with advanced-stage metastatic breast and lung cancers. The device also demonstrates high specificity and consistency, showing a further improvement and yield over our previous integrated biochip.[26] (iii) *Viable CTC collection*: unlike affinity-based, electrical or physical filtration platforms, the continuous collection of higher enriched populations of CTCs and short residence time in the micro-channels (<10 ms) eliminates the long-shear exposure to the CTCs, hence minimizing any undesirable phenotype changes due to the shear stress. The enriched cells are continuously collected in a separate tube in real time and can be used for high-definition imaging as well as RNA-based single-cell molecular analysis. (iv) *Affordability*: our device uses simple microfluidic channels, which can be produced at low-cost using conventional microfabrication techniques. In addition, it only needs two plastic syringes for sheath and sample loading into the biochip. Further improvement will come in the form of an automated system capable of blood handling and processing. Moreover, a critical advantage of this biochip is the ability to return all fractions of blood – plasma, CTCs and peripheral blood mononucleated cells (PBMCs) – that can be utilized for other diverse biomarker studies.

Conclusions

We demonstrated the high-throughput and high-resolution separation of CTCs from blood using a multiplexed spiral

microfluidic device. This approach utilizes the combined effect of inertial and Dean drag force to separate rare cells from a large volume of blood samples rapidly and efficiently. The label-free nature of the spiral biochip has improved the yield of CTC capture in certain diseases like lung cancer, and current research can now be further directed at culturing viable CTCs, performing single cell analysis including next generation sequencing and RNA-seq as well as the improving scalability in terms of detecting clinically-actionable genetic alterations.

Acknowledgements

We would like to express our sincere gratitude to all patients who participated in this trial and the healthy volunteers who donated blood samples for characterization of our device. Financial support by the Singapore–MIT Alliance for Research and Technology (SMART) Centre (BioSyM IRG) is gratefully acknowledged. This work is also supported by the use of NTU's Micro-Machine Center (MMC) facilities for wafer fabrication and the lab facilities at the Mechanobiology Institute (MBI) and the Nano Biomechanics Laboratory at the National University of Singapore. The clinical samples and data collection were supported by the Singapore National Medical Research Council grant NMRC 1225/2009.

References

1 K. Pantel, R. H. Brakenhoff and B. Brandt, *Nat. Rev. Cancer*, 2008, **8**, 329–340.
2 D. R. Parkinson, N. Dracopoli, B. G. Petty, C. Compton, M. Cristofanilli, A. Deisseroth, D. F. Hayes, G. Kapke, P. Kumar and J. S. H. Lee, *J. Transl. Med.*, 2012, **10**, 138.
3 M. Yu, S. Stott, M. Toner, S. Maheswaran and D. A. Haber, *J. Cell Biol.*, 2011, **192**, 373–382.
4 Y. F. Sun, X. R. Yang, J. Zhou, S. J. Qiu, J. Fan and Y. Xu, *J. Cancer Res. Clin. Oncol.*, 2011, **137**, 1–23.
5 W. He, H. Wang, L. C. Hartmann, J. X. Cheng and P. S. Low, *Proc. Natl. Acad. Sci. U. S. A.*, 2007, **104**, 11760.
6 R. Gertler, R. Rosenberg, K. Fuehrer, M. Dahm, H. Nekarda and J. Siewert, *Recent Results Cancer Res.*, 2003, **162**, 149–156.
7 A. L. Allan, S. A. Vantyghem, A. B. Tuck, A. F. Chambers, I. H. Chin-Yee and M. Keeney, *Cytometry, Part A*, 2005, **65**, 4–14.
8 I. Cruz, J. J. Cruz, M. Ramos, A. Gómez-Alonso, J. C. Adansa, C. Rodríguez and A. Orfao, *Am. J. Clin. Pathol.*, 2005, **123**, 66–74.
9 B. Khoo, M. Warkiani, G. Guan, D. S.-W. Tan, A. S. Lim, W.-T. Lim, Y. S. Yap, S. C. Lee, R. A. Soo and J. Han, *Ultra-High Throughput Enrichment of Viable Circulating Tumor Cells*, The 15th International Conference on Biomedical Engineering, 2014, pp. 1–4.
10 S. Nagrath, L. V. Sequist, S. Maheswaran, D. W. Bell, D. Irimia, L. Ulkus, M. R. Smith, E. L. Kwak, S. Digumarthy, A. Muzikansky, P. Ryan, U. J. Balis, R. G. Tompkins, D. A. Haber and M. Toner, *Nature*, 2007, **450**, 1235–1239.
11 S. L. Stott, C. H. Hsu, D. I. Tsukrov, M. Yu, D. T. Miyamoto, B. A. Waltman, S. M. Rothenberg, A. M. Shah, M. E. Smas and G. K. Korir, *Proc. Natl. Acad. Sci. U. S. A.*, 2010, **107**, 18392–18397.
12 S. Mittal, I. Y. Wong, W. M. Deen and M. Toner, *Biophys. J.*, 2012, **102**, 721–730.
13 C. Alix-Panabières, H. Schwarzenbach and K. Pantel, *Annu. Rev. Med.*, 2012, **63**, 199–215.
14 V. Gupta, I. Jafferji, M. Garza, V. O. Melnikova, D. K. Hasegawa, R. Pethig and D. W. Davis, *Biomicrofluidics*, 2012, **6**, 024133.
15 E. Ozkumur, A. M. Shah, J. C. Ciciliano, B. L. Emmink, D. T. Miyamoto, E. Brachtel, M. Yu, P.-i. Chen, B. Morgan and J. Trautwein, *Sci. Transl. Med.*, 2013, **5**, 179ra147.
16 H. S. Moon, K. Kwon, S. I. Kim, H. Han, J. Sohn, S. Lee and H. I. Jung, *Lab Chip*, 2011, **11**, 1118–1125.
17 E. W. Majid and C. T. Lim, in *Materiomics: Multiscale Mechanics of Biological Materials and Structures*, Springer, 2013, pp. 107–119.
18 J. Chen, J. Li and Y. Sun, *Lab Chip*, 2012, **12**, 1753–1767.
19 A. Sabile, G. Vona, M. Louha, V. Sitruk, S. Romana, K. Schütze, F. Capron, D. Franco, M. Pazzagli, M. Vekemans, B. Lacour, C. Bréchot and P. Paterlini-Bréchot, *Am. J. Pathol.*, 2000, **156**, 57–63.
20 S. Zheng, H. K. Lin, A. J. Williams, M. Balic, S. Groshen, H. I. Scher, M. Fleisher, W. Stadler, R. H. Datar, Y. C. Tai and R. J. Cote, *Clin. Cancer Res.*, 2010, **16**, 5011–5018.
21 J. D. Esinhart, T. K. Lee, L. D. Blackburn and J. F. Silverman, *Anal. Quant. Cytol. Histol.*, 1992, **14**, 32–34.
22 S. J. Tan, L. Yobas, G. Y. H. Lee, C. N. Ong and C. T. Lim, *Biomed. Microdevices*, 2009, **11**, 883–892.
23 M. E. Warkiani, C.-P. Lou and H.-Q. Gong, *Biomicrofluidics*, 2011, **5**, 036504.
24 A. A. S. Bhagat, H. Bow, H. W. Hou, S. J. Tan, J. Han and C. T. Lim, *Med. Biol. Eng. Comput.*, 2010, **48**, 999–1014.
25 E. W. Majid, G. Guan, B. L. Khoo, W. C. Lee, A. A. S. Bhagat, D. S.-W. Tan, W. T. Lim, S. C. Lee, P. C. Chen and C. T. Lim, *Lab Chip*, 2014, **14**, 128–137.
26 H. W. Hou, M. E. Warkiani, B. L. Khoo, Z. R. Li, R. A. Soo, D. S.-W. Tan, W.-T. Lim, J. Han, A. A. S. Bhagat and C. T. Lim, *Sci. Rep.*, 2013, **3**, 1259.
27 Y. Xia and G. M. Whitesides, *Annu. Rev. Mater. Sci.*, 1998, **28**, 153–184.
28 M. E. Warkiani, A. A. S. Bhagat, B. L. Khoo, J. Han, C. T. Lim, H. Q. Gong and A. G. Fane, *ACS Nano*, 2013, **7**, 1882–1904.
29 A. A. S. Bhagat, S. S. Kuntaegowdanahalli and I. Papautsky, *Lab Chip*, 2008, **8**, 1906–1914.
30 S. K. Arya, B. Lim and A. R. A. Rahman, *Lab Chip*, 2013, **13**, 1995–2027.
31 W. C. Lee, A. A. S. Bhagat, S. Huang, K. J. Van Vliet, J. Han and C. T. Lim, *Lab Chip*, 2011, **11**, 1359–1367.
32 G. M. Clark, D. J. Slamon, S. G. Wong, W. J. Levin, A. Ullrich and W. L. McGuire, *Science*, 1987, **235**, 177–182.
33 W. Godolphin, D. J. Slamon, L. A. Jones, J. A. Holt, S. G. Wong, D. E. Keith, W. J. Levin, S. G. Stuart, J. Udove, A. Ullrich and F. P. Michael, *Science*, 1989, **244**, 707–712.

34 S. Riethdorf, V. Müller, L. Zhang, T. Rau, S. Loibl, M. Komor, M. Roller, J. Huober, T. Fehm and I. Schrader, *Clin. Cancer Res.*, 2010, **16**, 2634–2645.
35 D. Marrinucci, K. Bethel, D. Lazar, J. Fisher, E. Huynh, P. Clark, R. Bruce, J. Nieva and P. Kuhn, *J. Oncol.*, 2010, **2010**, 1–7.
36 C. Kahlert, H. Weber, C. Mogler, F. Bergmann, P. Schirmacher, H. Kenngott, U. Matterne, N. Mollberg, N. Rahbari and U. Hinz, *Br. J. Cancer*, 2009, **101**, 457–464.
37 A. Lugli, G. Iezzi, I. Hostettler, M. Muraro, V. Mele, L. Tornillo, V. Carafa, G. Spagnoli, L. Terracciano and I. Zlobec, *Br. J. Cancer*, 2010, **103**, 382–390.